ELSEVIER

Journal of Chromatography A, 688 (1994) 273–282

JOURNAL OF CHROMATOGRAPHY A

Effects of pH and hydroxypropyl β-cyclodextrin concentration on peak resolution in the capillary electrophoretic separation of the enantiomers of weak bases

Yasir Y. Rawjee[1], Robert L. Williams, Lisa A. Buckingham[2], Gyula Vigh*

Chemistry Department, Texas A & M University, College Station, TX 77843-3255, USA

First received 28 June 1994; revised manuscript received 12 September 1994

Abstract

Weak base enantiomers were separated by capillary electrophoresis using hydroxypropyl β-cyclodextrin-containing background electrolytes. The multiple equilibria-based electrophoretic separation selectivity model (DID model) of enantiomers was used to analyze the results and determine the model parameters. The extended peak resolution equation of capillary electrophoresis has been applied to calculate the peak resolution surfaces as a function of the pH and the hydroxypropyl β-cyclodextrin concentration of the background electrolyte, the dimensionless electroosmotic flow coefficient, and the effective portion of the applied potential. Combination of the DID selectivity model and the extended peak resolution equation allows the rational optimization of the operating conditions and the realization of separations previously deemed impossible.

1. Introduction

By considering the pertinent multiple equilibria, an equation has been derived [1,2] to express selectivity in the CE separation of the enantiomers of weak bases as a function of the pH and the chiral resolving agent (hydroxypropyl β-cyclodextrin, HP-β-CD) concentration of the background electrolyte (BGE):

$$\alpha_{R/S} = \frac{\mu^0_+ - \mu^0_{HRCD^+} \cdot K_{HRCD^+}[CD]}{\mu^0_+ + \mu^0_{HSCD^+} \cdot K_{HSCD^+}[CD]} \cdot \frac{1 + K_{HSCD} \cdot [CD] + \frac{[OH^-]}{K_b} \cdot (1 + K_{SCD}[CD])}{1 + K_{HRCD} \cdot [CD] + \frac{[OH^-]}{K_b} \cdot (1 + K_{RCD}[CD])} \quad (1)$$

where subscripts R and S describe the two enantiomers, + is shorthand notation for the dissociated weak base enantiomers, HR^+ and HS^+, which are not complexed with HP-β-CD, RCD and SCD, and $HRCD^+$ and $HSCD^+$ stand for the non-dissociated and dissociated weak base enantiomers which are complexed with HP-β-CD, μ^0_+, $\mu^0_{HRCD^+}$ and $\mu^0_{HSCD^+}$ are the ionic mobilities of the free and the complexed enantiomers, K_b is the base dissociation constant of the enantiomers, and K_{RCD}, K_{SCD}, K_{HRCD^+} and

* Corresponding author.

[1] Present address: Smith-Kline Beecham, King of Prussia, PA 19406, USA.

[2] Present address: Department of Chemistry, Sweet Briar College, VA 24595, USA.

0021-9673/94/$07.00
SSDI 0021-9673(94)00888-4

K_{HSCD^+} are the formation constants for the respective enantiomer–HP-β-CD complexes, and [CD] and [OH^-] are the molar concentrations of HP-β-CD and hydroxyl ion in the BGE. If the analytical concentration of the analyte is much smaller than that of the HP-β-CD, [CD] can be considered identical to the analytical concentration of HP-β-CD. (For the sake of discussion, it is assumed that in the presence of cyclodextrin the mobility of the *S* enantiomer is smaller than that of the *R* enantiomer.)

The model parameters (K_b, $\mu^0_{a^-}$, $\mu^0_{HRCD^+}$, $\mu^0_{HSCD^+}$, K_{RCD}, K_{SCD}, K_{HRCD^+} and K_{HSCD^+}) can be easily calculated from the electroosmotic flow-corrected effective mobilities of the enantiomers, measured in three sets of BGEs. The first set of measurements is carried out in the absence of CD: the pH of the BGE is varied, but the ionic strength is kept constant at a preselected value [3]. In the second set, pH is kept constant at least 1 (preferably, 2) pH units below the pK_a of the conjugate acid enantiomers, and [CD] is varied while the ionic strength is kept constant at the preselected value. Finally, in the third set of experiments, pH is kept constant at about 0.5 pH units above the pK_a of the conjugate acid enantiomers, and [CD] is varied while the ionic strength is kept constant at the preselected value. In each run, the coefficient of the electroosmotic flow is also determined by simultaneous injection of a non-charged component (e.g. benzyl alcohol). The effective mobility data are then analyzed using a non-linear least square approach.

It was recognized in Refs. [1] and [2] that three different types of CE enantiomer separations exist, depending on the numeric values of the model parameters. The separation in which only the non-charged forms of the analytes interact selectively with the resolving agent (i.e. $K_{RCD} \neq K_{SCD}$), has been called a *Type I* separation. In order to have a more descriptive name, it is suggested that such separations be called *desionoselective* CE separations. The separation in which only the charged forms of the analytes interact selectively with the resolving agent (i.e. $K_{HRCD^+} \neq K_{HSCD^+}$), has been called a *Type II* separation. It is suggested that such separations be called *ionoselective* CE separations. Finally, the separation in which both the charged and the non-charged forms of the analytes interact selectively with the resolving agent (i.e. $K_{RCD} \neq K_{SCD}$ and $K_{HRCD^+} \neq K_{HSCD^+}$), has been called a *Type III* separation. The recommended term for such a separation is *duoselective* CE separation. The selectivity model itself will be referred to as DID selectivity model.

An equation has been introduced [3,4] to express peak resolution in the CE separation of enantiomers as a function of the separation selectivity, α, the dimensionless electroosmotic flow coefficient, β, and the effective charge of the enantiomers, z_R^{eff}, z_S^{eff}:

$$R_s = \sqrt{\frac{Ele_0}{8kT}} \cdot \frac{\text{abs}(\alpha - 1) \cdot \sqrt{\text{abs}(\alpha + \beta)} \cdot \sqrt{\text{abs}(1 + \beta)} \cdot \sqrt{z_R^{eff}} \cdot \sqrt{z_S^{eff}}}{\sqrt{\text{abs}[(\alpha + \beta)^3] z_R^{eff}} + \sqrt{\alpha \ \text{abs}[(1 - \beta)^3] z_S^{eff}}} \quad (2)$$

where E is the field strength, l the length of the capillary from injector to detector, e_0 the electric charge, k the Boltzman constant and T the absolute temperature. In this expression, the dimensionless coefficient of the electroosmotic flow, β, is defined as:

$$\beta = \frac{\mu_{eo}}{\mu_S^{eff}} \quad (3)$$

with

$$\mu_S^{obs} = \mu_S^{eff} + \mu_{eo} \quad (4)$$

where μ_S^{obs} is the observed mobility of the *S* enantiomer, μ_S^{eff} is the effective mobility of the *S* enantiomer and μ_{eo} is the coefficient of the electroosmotic flow. According to Refs. [1] and [2], μ_S^{eff} is:

$$\mu_S^{eff} = \frac{\mu^0_{HS^+} + \mu^0_{HSCD^+} K_{HSCD^+}[CD]}{1 + K_{HSCD^+}[CD] + \frac{[OH^-]}{K_b} \cdot (1 + K_{SCD}[CD])} \quad (5)$$

while according to Refs. [3] and [4], the effective charge of the S enantiomer, z_S^{eff}, is:

$$z_S^{eff} = \frac{z^0_{S^-} + z^0_{HSCD^-} \cdot K_{HSCD} \cdot [CD]}{1 + K_{HSCD} \cdot [CD] + \frac{[OH^-]}{K_b} \cdot (1 + K_{SCD}[CD])} \quad (6)$$

with $z^0_{HS^-}$ and $z^0_{HSCD^-}$ as the ionic charges of the fully dissociated enantiomers, non-complexed and complexed, respectively. Similar expressions exist for the R enantiomer.

The objective of this paper is to show that peak resolution for the enantiomers of weak bases is an explicit function of both the pH and the HP-β-CD concentration of the background electrolyte, as well as the dimensionless electroosmotic flow. Knowledge of the unique resolution surfaces that belong to the ionoselective, desionoselective and duoselective separation types allow the rational optimization of the separation conditions and the realization of the CE separations of weak base enantiomers which were previously considered impossible.

2. Experimental

A P/ACE 2100 system (Beckman Instruments, Fullerton, CA, USA) was used for all measurements, with its UV detector set at 200 nm and the thermostatting liquid bath temperature maintained at 25°C. The electrode at the injection end of the capillary was kept at high positive potential; the electrode at the detector end of the capillary was at ground potential. The field strength was varied between 150 and 750 V/cm to keep the power dissipation at 95 mW. The 0.1–0.2 mM samples (which also contained benzyl alcohol as electroosmotic flow marker) were injected electrokinetically. Untreated, 45.5 cm (39.5 cm from injector to detector) × 25 μm I.D. × 150 μm O.D. fused-silica capillaries (Polymicro Technologies, Phoenix, AZ, USA) and 39.7 cm (33.2 cm from injector to detector) × 75 μm I.D. × 375 μm O.D. fused-silica capillaries with a neutral coating (Beckman Instruments) were used.

HP-β-CD (average degree of substitution of 7 [3]) was synthesized according to the modified procedure of Rao et al. [5] from β-cyclodextrin (American Maize Products, Hammond, IN, USA). BGE components 3-[tris(hydroxymethyl)-methylamino]-1-propanesulfonic acid (TAPS) and 3-(cyclohexylamino)-2-hydroxy-1-propanesulfonic acid (CAPSO) were obtained from Sigma (St. Louis, MO, USA), methanesulfonic acid (MSA) from Aldrich (Milwaukee, WI, USA), Jeffamine ED-600 from Texaco (Houston, TX, USA), and 250MHR PA hydroxyethyl cellulose (HEC) from Aqualon (Wilmington, DE, USA). Test solutes atropine, chloroamphetamine, propranolol and benzyltrimethylammonium bromide (BTM^+) were obtained from Sigma. α-(Hydroxymethyl)benzyltriethylammonium chloride ($HBTEA^+$) was synthesized in our laboratory according to Ref. [6].

All solutions were freshly prepared using deionized water from a Milli-Q unit (Millipore, Milford, MA, USA). Irrespective of the pH of the BGE, the anion concentration was maintained constant at 100 mM. The anion-concentration balanced background electrolytes [3] were prepared by adding an accurately measured volume of the concentrated stock solution of the buffer, accurately weighed amounts of Jeffamine ED-600, HP-β-CD, ionic strength controlling agent MSA and an accurately measured volume of the concentrated stock solution of HEC to a volumetric flask [3]. The flask was filled to 95% of its capacity with deionized water and the contents mixed thoroughly. The pH of the solution was then adjusted using a concentrated solution of lithium hydroxide or 40% tetrabutylammonium hydroxide solution. Subsequently, the volume was made up to the mark with deionized water. The BGE was degassed prior to loading into the electrolyte reservoirs. Before each series of measurements, the capillary was washed with 0.1 M NaOH, rinsed by deionized water and equilibrated with the background electrolyte (5 min, 5 min and 15 min,

respectively). Each run was repeated in at least triplicate.

The parameters in Eqs. 1, 5 and 6 were estimated from the measured, electroosmotic flow-corrected effective mobilities using the Table Curve 3D software package (Jandell, San Raffael, CA, USA) running on a 486DX2 66 MHz 16M RAM personal computer (Computer Access, College Station, TX, USA). Eq. 5 was rewritten as user defined function in the *.udf format of the Table Curve 3D software package and the μ^0 and K values were obtained as parameters. Once the parameters were determined, the three-dimensional surfaces were calculated using the Origin Version 3.0 software package (MicroCal, Northampton, MA, USA).

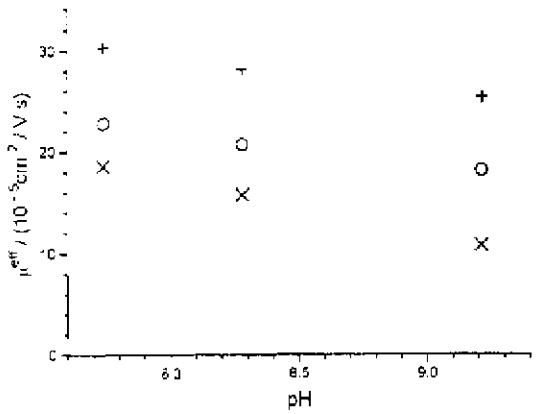

Fig. 1. Effective mobility of propranolol (+), $HBTEA^+$ (○), and BTM^+ (×) in 100 m*M* TAPS buffers as a function of the BGE pH, adjusted by tetrabutylammonium hydroxide.

3. Results and discussion

3.1. Determination of the model parameters

In order to determine the base dissociation constant and ionic mobility of a weak base, one can change the pH of the BGE around the expected pK_b value and measure the effective mobilities of the solute [7]. To obtain correct pK_b values, the observed effective mobility change must be due to the change in the solute charge only. One can ascertain that this premise is fulfilled by adding a permanent cation probe, such as BTM^+ or $HBTEA^+$, to the sample. If the effective mobilities of the permanent cation remain constant while the pH of the BGE is changed, the effective mobility values of the simultaneously electrophoresed weak base can be used for the pK_b determinations. If one prepares the BGE in the conventional way, e.g. starting with a 100 m*M* TAPS ($pK_a = 8.4$) solution and varying its pH from 7.5 to 9.5 by adding increasing amounts of tetrabutylammonium hydroxide, and then uses these BGEs to determine the effective mobilities, one obtains results similar to those shown in Fig. 1. Clearly, the effective mobilities of both the weak base solute (propranolol, symbol +) and the permanent cations (BTM^+, symbol × and $HBTEA^+$, symbol ○), decrease significantly. This large mobility decrease is due to the fact that the anion concentration (counter-ion concentration) increases drastically as pH is increased (from about 2 m*M* at pH 6.75 to about 99 m*M* at pH 10.5). Therefore, to keep the anion concentration constant, a non-hydrolyzing anion, e.g. methanesulfonate (MSA^-), must be added to the BGE in decreasing concentrations as the pH is increased. Such BGEs are called counter-ion concentration-balanced BGEs [3] and can be prepared as described in the Experimental section for weak base analytes, and in Ref. [3], for weak acid analytes.

The K_b and μ_+^0 values of the weak base test solutes were determined using counter-ion concentration-balanced BGEs. In the $7.1 < pH < 9.5$ range these BGEs contained 100 m*M* TAPS and 20 m*M* Jeffamine ED-600; in the $9.3 < pH < 10.1$ range they contained 100 m*M* CAPSO ($pK_a = 9.6$) and 20 m*M* Jeffamine ED-600. The final pH adjustment was made with a small amount of tetrabutylammonium hydroxide solution. BTM^+ and $HBTEA^+$ were added to the samples as permanently cationic mobility markers. As an example, the effective mobilities of atropine are plotted in Fig. 2a as a function of the pH of the BGE. With counter-ion concentration balancing [3], the mobilities of the permanent cation, $HBTEA^+$, indeed become constant. The calculated K_b and μ_+^0 values of the weak base test

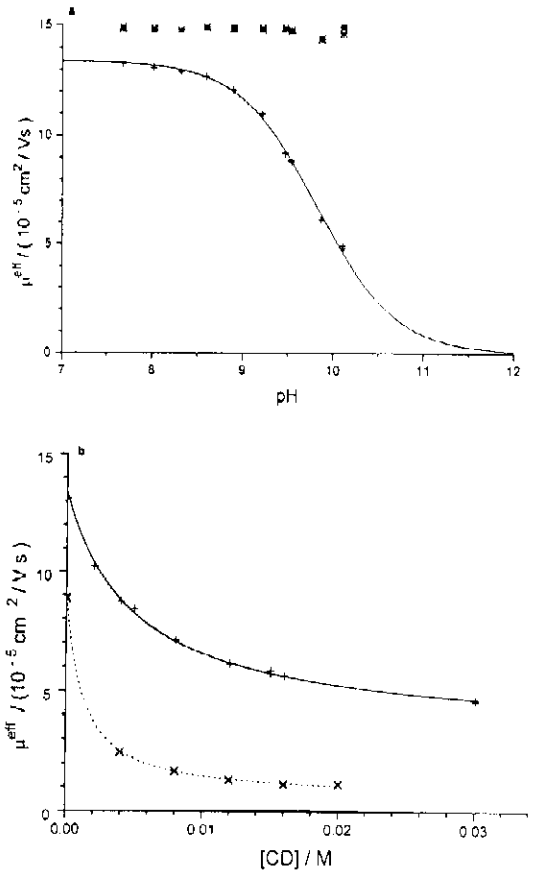

Fig. 2. Effective mobility of atropine (+) and HBTEA$^+$ (*) in counter-ion concentration balanced 100 m*M* TAPS buffers as a function of (a) the pH of the BGE, (b) the HP-β-CD concentration of the BGE at pH 7.63 (top curve), and at pH 9.5 (bottom curve). Solid lines: best fit curves calculated with the constants listed in Table 1.

solutes determined from these measurements are listed in Table 1.

Next, the effects of the HP-β-CD concentration were tested in a low-pH TAPS background electrolyte, in which the weak base analytes are almost completely dissociated (pH 7.63). Again, as an example, the effective mobilities of atropine are plotted in Fig. 2b as a function of [CD] in the BGE. Finally, the effects of the HP-β-CD concentration were tested in a high-pH TAPS background electrolyte, in which the weak base analytes are about 50% dissociated (pH 9.5). Again, as an example, the effective mobilities of the less mobile enantiomer of atropine are plotted in Fig. 2b as a function of [CD]. The calculated $\mu^0_{HRCD^+}$, $\mu^0_{HSCD^+}$, K_{HRCD^+}, K_{HSCD^+}, K_{RCD} and K_{SCD} values of the weak base test substances are listed in Table 1.

Since the complex formation constants of the protonated atropine enantiomers are identical, i.e. $K_{HRCD^+} = K_{HSCD^+} = 211$, this separation represents a desionoselective separation (a Type I separation, in the old nomenclature [1–3]). Since the complex formation constants of the non-protonated chloroamphetamine enantiomers are identical within the experimental error ($K_{RCD} = 1000$ and $K_{SCD} = 1006$), this separation represents an ionoselective separation (a Type II separation, in the old nomenclature). For propranolol, none of the complex formation constants are identical, $K_{HRCD^+} \neq K_{HSCD^+}$ and $K_{RCD} \neq K_{SCD}$. Therefore, this separation represents a duoselective separation (a Type III sepa-

Table 1
Estimated model parameter values for the chiral week bases

Parameter	Atropine	Chloroamphetamine	Propranolol
μ^0_+ (10^{-5} cm^2/V s)	13.40 + 0.06	17.5 ± 0.1	12.4 ± 0.1
$10^5 K_b$	6.62 + 0.03	5.65 ± 0.05	2.9 ± 0.1
pK_a	9.82	9.75	9.47
$\mu^0_{HRCD^+}$ (10^{-5} cm^2/V s)	3.3 + 0.1	3.3 ± 0.1	3.2 ± 0.1
$\mu^0_{HSCD^+}$ (10^{-5} cm^2/V s)	3.3 + 0.1	3.4 ± 0.1	3.2 ± 0.1
$K^0_{HRCD^+}$	211 + 8	140 ± 4	108 ± 3
$K^0_{HSCD^+}$	211 + 8	148 ± 4	116 ± 3
K_{RCD}	2140 + 60	1000 ± 40	148 ± 5
K_{SCD}	2320 ± 60	1000 ± 40	163 ± 5

ration, in the old nomenclature). Since all the parameters used in the effective mobility, effective charge, separation selectivity and peak resolution equations are known, the respective surfaces for the three separation types can be calculated and studied.

The general appearance of the z^{eff} and μ^{eff} surfaces are similar for all test solutes, except that the curvature of the surfaces along the HP-β-CD concentration axis varies, depending on the magnitude of the K_{HRCD^+}, K_{HSCD^+}, K_{RCD} and K_{SCD} constants: the greater the constant values, the sharper the initial decrease as [CD] is increased. As examples, the effective charge surface and the effective mobility surface of the less mobile enantiomer of atropine as a function of pH and [CD] are shown in Fig. 3a and b.

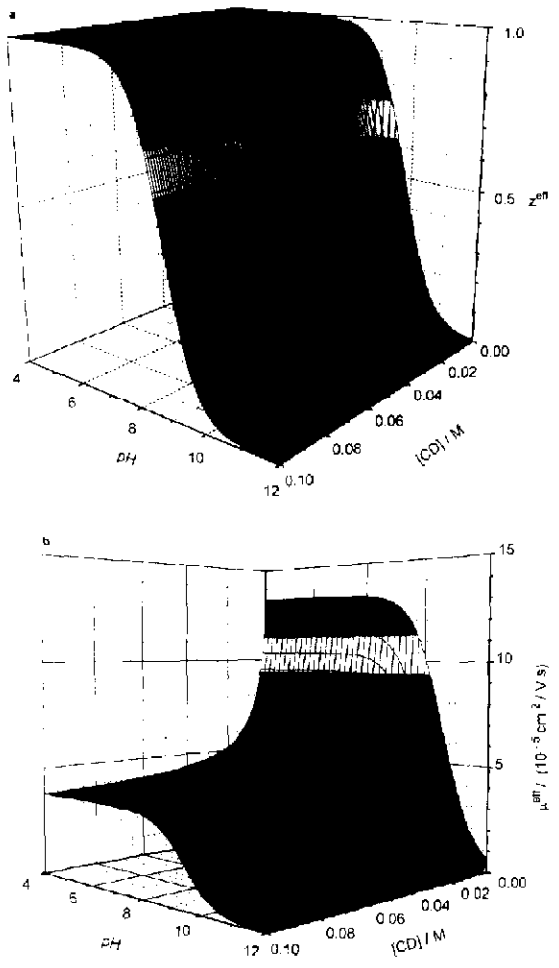

Fig. 3. The dependence of the (a) effective charge and (b) effective mobility of the less mobile enantiomer of atropine as a function of the HP-β-CD concentration and the pH in counter-ion concentration balanced 100 mM TAPS BGEs. The surfaces were calculated with Eq. 6 (charge), Eq. 5 (mobility) and the constants in Table 1.

3.2. Separation selectivity surfaces

The three-dimensional separation selectivity surfaces for atropine, chloroamphetamine and propranolol are shown in Fig. 4 (with the contour plots on the bottom plane) as a function of pH and [CD]. For atropine, selectivity increases from unity at low pH and low [CD] to a limiting high value at high pH and high [CD]. This behavior is typical of desionoselective weak base enantiomer separations (Fig. 4a). For chloroamphetamine at low pH, α increases rapidly as [CD] is increased (Fig. 4b), passes a maximum at about [CD] = 15 mM, then slowly decreases as [CD] is increased further. Along the pH axis, at [CD] $\approx$ 15 mM, α remains a constant high value as long as pH $< pK_a - 2$, then decreases rapidly, crosses the $\alpha = 1$ plane and continues to decrease as pH is increased further. This means that the migration order of the enantiomers can be reversed by selecting the right combination of pH and [CD]. This behavior is typical of ionoselective separations of weak base enantiomers. For propranolol (Fig. 4c), α again passes a maximum as [CD] is increased at both low and high pH, then drops below unity at low pH as [CD] is increased further. This means that the migration order of the enantiomers can be reversed at low pH by greatly increasing [CD]. This behavior is typical of duoselective separations. Along the pH axis, at [CD] $\approx$ 15 mM, α remains constant as long as pH $< pK_a - 2$, then increases to a limiting value in the pH $> pK_a + 1$ range.

3.3. Peak resolution surfaces

The peak resolution surfaces can be calculated with Eq. 2. However, since R_s depends on pH, [CD] and β, the dimensionless electroosmotic flow coefficient, one of these variables must be

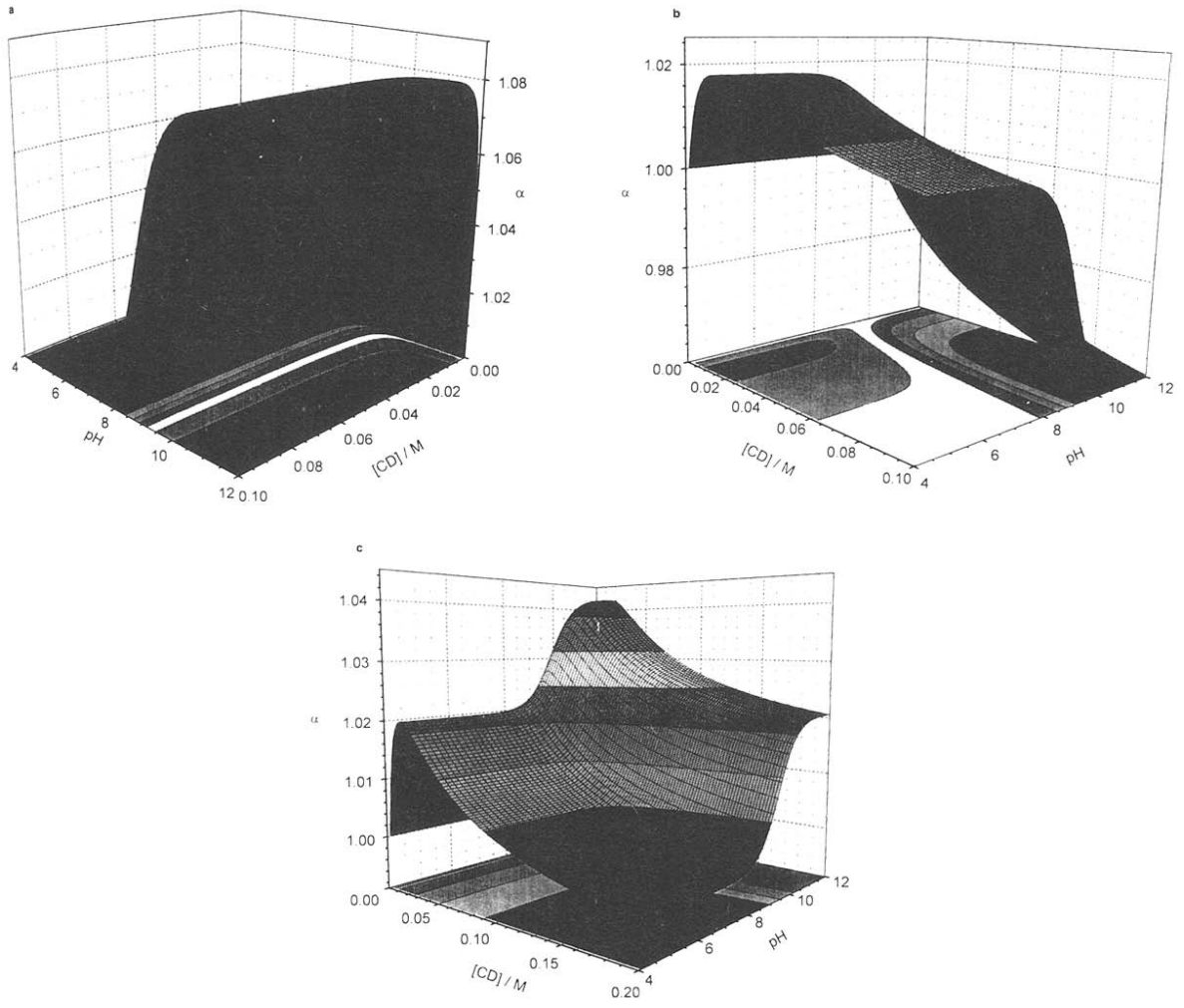

Fig. 4. Selectivity surfaces for the separation of the enantiomers of (a) atropine (desionoselective separation), (b) chloroamphetamine (ionoselective separation) and (c) propranolol (duoselective separation) as a function of the HP-β-CD concentration and the pH in counter-ion concentration balanced 100 m*M* TAPS BGEs. The surfaces were calculated with Eq. 1 and the constants in Table 1.

held constant if the surfaces are to be visualized. For Fig. 5, where R_s is shown as a function of pH and [CD] for atropine, chloroamphetamine and propranolol, we selected $\beta = 0$ (i.e. no electroosmotic flow). This condition can be realized easily by using capillaries with a hydrophilic, neutral coating. For the desionoselective separation shown in Fig. 5a (atropine), resolution can only be achieved over a narrow pH range, about 2 pH units wide, in the vicinity of the pK_a value. This means that desionoselective separations are not rugged in terms of the pH variable. This may be the main reason why previous attempts to separate the enantiomers of atropine [8] proved unsuccessful. On the [CD] axis, resolution barely changes once the HP-β-CD concentration exceeds 20 m*M*, i.e. the separation is quite rugged in terms of the [CD] variable.

For the ionoselective separation shown in Fig. 5b (chloroamphetamine), the resolution surface has two lobes. The primary lobe is at low pH, where the separation is rugged in terms of the pH variable (as long as it is at least 1.5 units below the pK_a), and not rugged in terms of

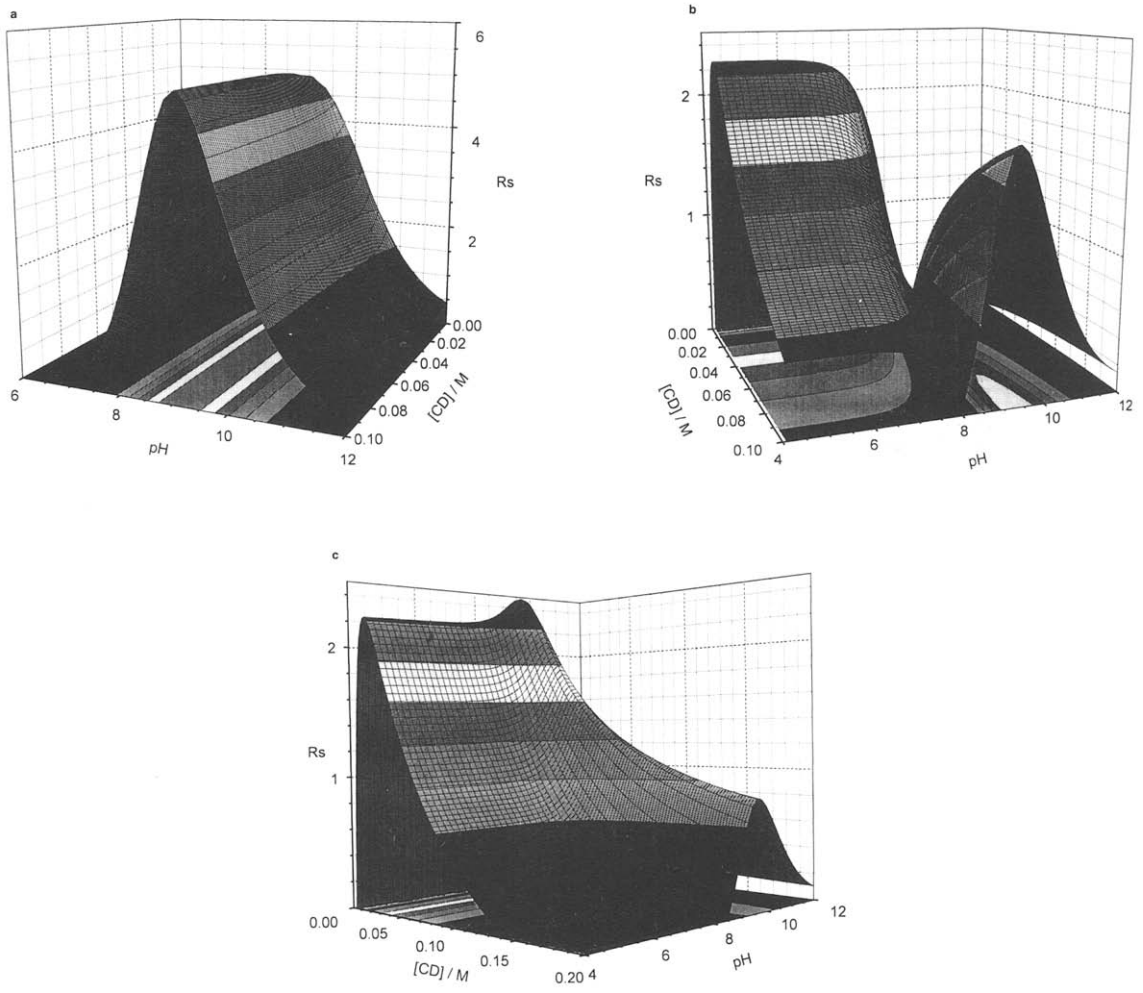

Fig. 5. Peak resolution surface for the separation of the enantiomers of (a) atropine (desionoselective separation), (b) chloroamphetamine (ionoselective separation) and (c) propranolol (duoselective separation) as a function of the HP-β-CD concentration and the pH in counter-ion concentration balanced 100 m*M* TAPS BGEs. The surface was calculated with Eq. 2 and the constants in Table 1 for $\beta = 0$ and $E = 329$ V/cm, $T = 298$ K and $l = 38.65$ cm.

[CD]. From a practical point of view, one is better off selecting a [CD] value that is slightly above the maximum point, because R_s changes here less rapidly than below the maximum point. The secondary lobe is at high pH. The migration order of the enantiomers on the secondary lobe is opposite to the one on the primary lobe. The separation is not rugged either in terms of pH or [CD].

For the duoselective separation shown in Fig. 5c (propranolol), the resolution surface again has two lobes. The primary one is at low [CD] and spans the entire pH range. The separation is rugged on the primary lobe in terms of pH, as long as it is about 1.5 units below the pK_a. Both the charged and the non-charged forms of the enantiomers of propranolol contribute to the separation cooperatively, because $K_{HRCD^+} < K_{HSCD^+}$ and $K_{RCD} < K_{SCD}$. Since K_{HSCD^+}/K_{HRCD^+} is smaller than K_{SCD}/K_{RCD} (1.07 vs. 1.10), R_s increases as pH is increased towards the pK_a value at [CD] ≈ 2 m*M*. A global R_s maximum is passed, then the resolution decreases rapidly due to the loss of charge at even

higher pH. The secondary lobe can be accessed more easily at low pH by increasing [CD] to high values. Just as in an ionoselective separation, the migration order of the enantiomers is opposite on the primary and the secondary lobes.

To show how closely the loci of the predicted and measured Rs maxima agree, and also, to demonstrate the importance of pH in a desionoselective separation, the electropherograms of atropine were determined at $E = 267$ V/cm using a 39.2/46.2 cm × 75 μm I.D. capillary with an experimental neutral coating (Beckman). The background electrolytes had a constant, 50 m*M* HP-β-CD concentration, and their pH was varied between 7.4 and 9.6. The measured (symbol ×) and the predicted (symbol +) R_s values are plotted as a function of pH in Fig. 6. The predicted R_s values were calculated with the constants in Table 1. The measured R_s values are only a third as high as the predicted ones, because electromigration dispersion leads to peak distortion. However, a baseline–baseline separation, shown in the inset in Fig. 6, can be achieved by simultaneously increasing the field strength to 378 V/cm and dynamically matching

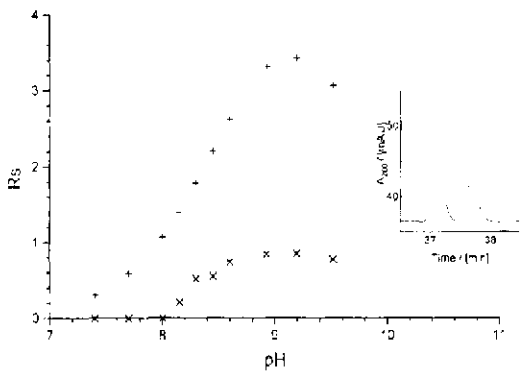

Fig. 6. Comparison of the predicted (+) and measured (×) R_s values for atropine as a function of pH in counter-ion concentration balanced 100 m*M* TAPS, [CD] = 50 m*M* BGEs. The measured values were obtained using a 33.2/39.7 cm × 75 μm I.D. capillary with a neutral coating (Beckman), $E = 267$ V/cm. Inset: partial electropherogram of a racemic mixture of atropine obtained in a counter-ion concentration balanced BGE with 50 m*M* TAPS, pH 8.6, [CD] = 50 m*M*, $E = 378$ V/cm, $T = 298$ K, $\beta < 0.1 \cdot 10^{-9}$ cm²/V s, using a 33.2/39.7 cm × 75 μm I.D. capillary with an experimental neutral coating (Beckman).

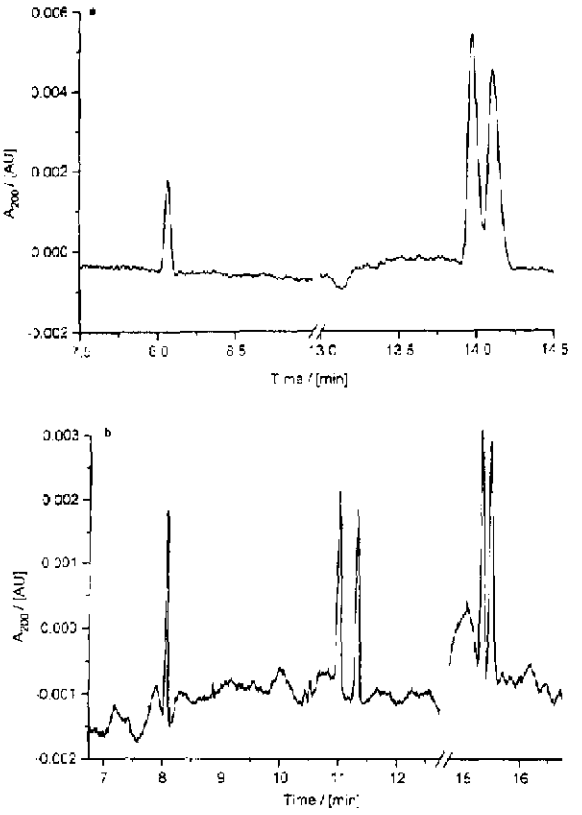

Fig. 7. Electropherograms of (a) BTM^+ and a racemic mixture of chloroamphetamine, and (b) BTM^+, racemic mixtures of $HBTEA^+$ and propranolol, obtained in a counter-ion concentration balanced 100 m*M* TAPS, pH 7.6, [CD] = 15 m*M* BGE, $E = 267$ V/cm, $T = 298$ K, $\beta < 0.1 \cdot 10^{-9}$ cm²/V s, using a 33.2/39.7 cm × 75 μm I.D. capillary with a neutral coating (Beckman).

the mobilities of the solutes and the BGE components (as described in Ref. [9]).

Finally, the electropherogram of a sample containing BTM^+ and a racemic mixture of chloroamphetamine is shown in Fig. 7a, while that of BTM^+ and racemic mixtures of $HBTEA^+$ and propranolol is shown in Fig. 7b.

4. Conclusions

The multiple equilibria-based DID selectivity model and the extended peak resolution equation of CE were used to analyze the possibilities of electrophoretic enantiomer separations for

chiral weak bases, using HP-β-CD as resolving agent. The existence of all three separation types predicted by theory has been verified experimentally for chiral weak bases. In a desionoselective separation (exemplified by atropine), only the non-dissociated enantiomers complex selectively, and resolution is possible only in a narrow pH range in the vicinity of the pK_a value. These separations are rugged in terms of the concentration of the resolving agent. In an ionoselective separation (exemplified by chloroamphetamine), only the dissociated enantiomers complex selectively. Resolution, displaying a local maximum as a function of the resolving agent concentration, is possible at any pH value that is at least two units below the pK_a. Resolution is also possible in the vicinity of the pK_a value, albeit at high resolving agent concentrations, and with a reversed migration order. Finally, in a duoselective separation (exemplified by propranolol), both the dissociated and the non-dissociated forms of the enantiomers complex selectively with the resolving agent. The resolution surface again has two lobes, affording different migration orders at different pH and resolving agent concentration combinations. The resolution equation explicitly shows the impressive resolution gains that can be realized by a judicial choice of the magnitude of the dimensionless electroosmotic flow coefficient. Combination of the extended peak resolution equation and the DID selectivity models permit the development of chiral CE separations in a methodical fashion, rather than by trial-and-error. Further work is under way in our laboratory to extend the model to other analytes and resolving agents as well.

Acknowledgements

Partial financial support by the National Science Foundation (CHE-8919151 and an NSF-REU fellowship to L.A.B.), the Texas Coordination Board of Higher Education Advanced Research Program (Project No. 010366-016), Beckman Instruments (Fullerton, CA, USA), the W.R. Johnson Pharmaceutical Research Institute (Springfield, PA, USA), and the Dow Chemical Company (Midland, MI, USA) is gratefully acknowledged. American Maize Products Corporation (Hammond, IN, USA) and the Aqualon Corporation (Wilmington, DE, USA), respectively, are acknowledged for the donation of the β-cyclodextrin and HEC samples. The authors are indebted to I. Cruzado for assistance with the atropine measurements.

References

[1] Y.Y. Rawjee, D.U. Staerk and Gy. Vigh, *J. Chromatogr.*, 635 (1993) 291.
[2] Y.Y. Rawjee, R.L. Williams and Gy. Vigh, *J. Chromatogr. A*, 652 (1993) 233.
[3] Y.Y. Rawjee and Gy. Vigh, *Anal. Chem.*, 66 (1994) 619.
[4] Y.Y. Rawjee, R.L. Williams and Gy. Vigh, *J. Chromatogr. A*, 680 (1994) 599.
[5] C.T. Rao, B. Lindberg, J. Lindberg and J. Pitha, *J. Org. Chem.*, 56 (1991) 1327.
[6] J.N. Kanazawa and N.S. Nishinomiya, *US Pat.*, 3 135 788 (1964).
[7] J.L. Beckers, F.M. Everaerts and M.T. Ackermans, *J. Chromatogr.*, 537 (1991) 407.
[8] M. Heuermann and G. Blaschke, *J. Chromatogr.*, 648 (1993) 267.
[9] Y.Y. Rawjee, R.L. Williams and Gy. Vigh, *Anal. Chem.*, 66 (1994) 3777.